E-proceedings of the 38th IAHR World Congress
September 1-6, 2019, Panama City, Panama
doi:10.3850/38WC092019-0143

A MOVABLE BED PHYSICAL MODEL YIELDS AN INNOVATIVE SOLUTION FOR REPLACING A FISH PASS SUFFERING FROM CLOGGING

VECSERNYES ZSOLT[1], WOHLWEND FLORENT [1], GOBAT KARINE[1] & ANDREINI NICOLAS[1]

[1] Geneva School of Engineering, Architecture and Landscape - HEPIA, HES-SO University of Applied Sciences and Arts Western Switzerland, Geneva, Switzerland

ABSTRACT

An experimental study carried out on a movable bed physical model at the Laboratory for Applied Hydraulics of HEPIA yielded an innovative solution to replace a fish pass suffering from clogging on the Arve River in Geneva. Fish migration in the Vessy meander is altered by a 220 m long, 3.5 m high spillway conveying a part of the river discharge to a low-head hydraulic power station. Since the Suisse Federal Law on Fishing (RS 923.0) requires from all power plant operators to guarantee a free fish migration the Service Industriel de Genève (SIG) is obliged to replace the inoperative fish pass. The main achievements of the investigations are a) calibration of the physical model to the current hydro- and morphodynamics; b) identification of the appropriate location of the fish entrance and the water intake of the future fish pass; c) hydraulic analyses of new structures; d) proposal of a sustainable and ecological solution. The analyses pointed out that a bypass river would gather the largest number of benefits. A concrete fish pass would suffer from clogging. A riprap ramp, although less exposed to clogging, would offer favourable hydraulic conditions only up to medium discharges of the Arve River. The bypass river would run on Arve's right overbank. Bed load is deflected by a groin implemented in the Arve upstream from the new water intake, protecting the latter from clogging. The new fish pass should offer optimal flow and ecological conditions for all fish species and can therefore be constructed.

Keywords: Physical hydraulic model, movable bed, clogging, fish pass, bypass river

1 INTRODUCTION

Fish migration is hindered in the Vessy meander of the Arve River by a 220 m long and 3.5 m high spillway erected in 1866 by the Société des eaux de l'Arve, fragmentising and isolating the habitats of fish populations. Over more than a century, this hydraulic structure conveyed a part of the river discharge to a pumping station in order to supply local municipalities of Geneva with drinking water. From 1966 until the completion of this activity in 1994, some 10 municipalities with 60'000 inhabitants became its beneficiary.

Figure 1 Aerial view of the Vessy meander of Arve, with the power plant, the inlet canal, the 220 m long and 3.5 high spillway and two fish passes implemented on the right bank and the central island (excerpt SITG).

In 1988 the Service Industriel de Genève (SIG) overtook these activities and constructed a low-head hydroelectric power plant to supply 650 households with electricity. A strainer implemented upstream from the plant reloads the groundwater, yielding drinking water supply indirectly. Two concrete fish passes were created, one implemented between the central island and the overflow weir of the plant, and the second embedded on the right riverbank (see Figure 1). An electric repulsive device installed in the plant's tailrace protects fishes migrating along the left riverbank. A kayak pass was created between the right-bank fish pass and the spillway.

River Arve is characterised by a strong sediment transport. The heavy annual suspended sediment discharge and bed load engender natural morphology in several reaches of Arve yielding alternate bars, point bars and local bed erosion. Downstream from de Vessy spillway, these patterns evolve due to successive flood and low-water conditions as shown in Figure 2. During flooding, also a large amount of wood is floated. These sediment and woody debris are responsible for failing of the Vessy fish passes, as shown in Figure 3.

Figure 2 The alluvial zone located downstream from the Vessy spillway shaped by the 100y flood of 2015.

Figure 3 Left: Right-bank fish pass clogged by sand, silt and woody debris, due to floods milder than annual.
Right: Central fish pass blocked by floated woods.

Given the high complexity of the hydraulic and sediment dynamic conditions of the Vessy meander the SIG mandated the Laboratory for Applied Hydraulics of HEPIA to study on a movable bed physical hydraulic model the replacement of the current right-bank fish pass. Feasibility analyses pointed out that a bypass river running on Arve's right overbank would offer optimal ecological and flow conditions. The present paper displays the related experimental-study achievements.

2 OBJECTIVES

Arve River offers with its tributaries favourable habitats for fish species. Since the Suisse Federal Law on Fishing (RS 923.0) requires from all hydraulic power plant operators to guarantee a free fish migration, the SIG is forced to replace the right-bank Vessy fish pass. The main objectives of the investigations carried out on a movable bed physical hydraulic model at HEPIA were:

a) Calibrate the physical model for observed hydraulics and morphodynamics of the Vessy meander
b) Identify the most relevant location of the fish entrance and water intake of the future bypass river
c) Analyse the comportment of the water intake from a hydrodynamic point of view
d) Explore structural measures in order to prevent the bypass river from clogging.

3 PRELIMINARY DATA

3.1 Hydrological data

The source of Arve River is situated in the Mont-Blanc mountain range. Its main stream extends over 95 km upstream from Geneva with a catchment area of 1976 km², defining an alpine nival hydrological regime. Arve River peak discharges were considered from Swiss Federal Office for the Environment (FOEN) statistical data.

Figure 4 presents the T-Q relationship due to high-water conditions (T return period; Q peak discharge). Figure *5* shows the T-Q relationship for low-water conditions (T return period; Q low-flow discharge).

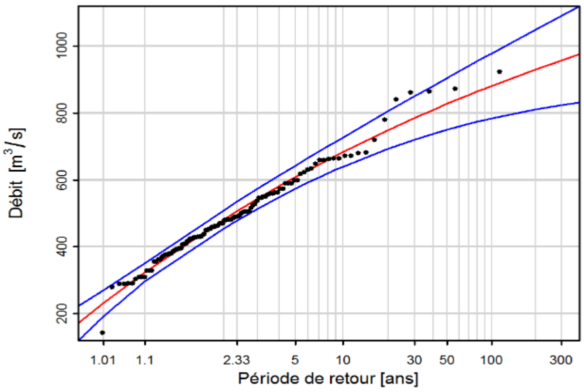

Table des niveaux de retour

Période de retour [ans]	Débit [m³/s]	Intervalle de confiance [m³/s]
2	482	455 - 509
10	683	640 - 726
30	785	720 - 850
100	881	783 - 978
300	957	823 - 1090

Table des extrema annuels les plus grands

Date	Débit [m³/s]	Période de retour estimée [ans]
02.05.2015	923	>150
06.08.1914	873	90
26.06.1910	865	81
24.12.1918	861	77
22.09.1968	840	59

Figure 4 High-water statistics of Arve River, at the Bout-du-monde station Geneva (FOEN)

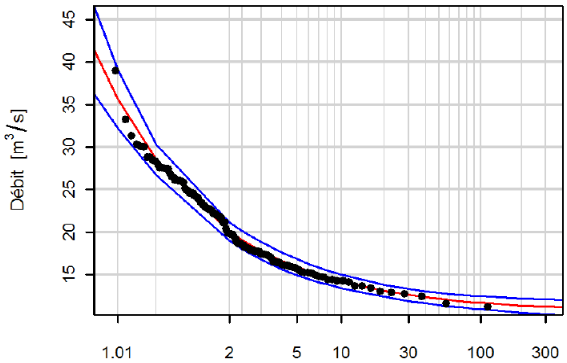

Table des niveaux de retour

Période de retour [ans]	Débit [m³/s]	Intervalle de confiance [m³/s]
2	20.1	21.3 - 18.8
10	14.2	15.1 - 13.3
30	12.6	13.4 - 11.8
100	11.7	12.6 - 10.8
300	11.2	12.2 - 10.2

Table des NM7Q les plus petits

Date NM7Q (±3 jours)	Débit [m³/s]	Période de retour estimée [ans]
29.11.2011	11.2	>150
05.03.1905	11.6	142
14.02.1942	12.4	40
09.12.1989	12.7	30
06.12.1962	12.9	25

Figure 5 Law-water statistics of Arve River, at the Bout-du-monde station Geneva (FOEN)

Recorded flood hydrograph time series for relevant return periods were obtained from FOEN Bout-du-monde station (cf. Figure 6). They served for simulation of hydrological conditions on the physical model.

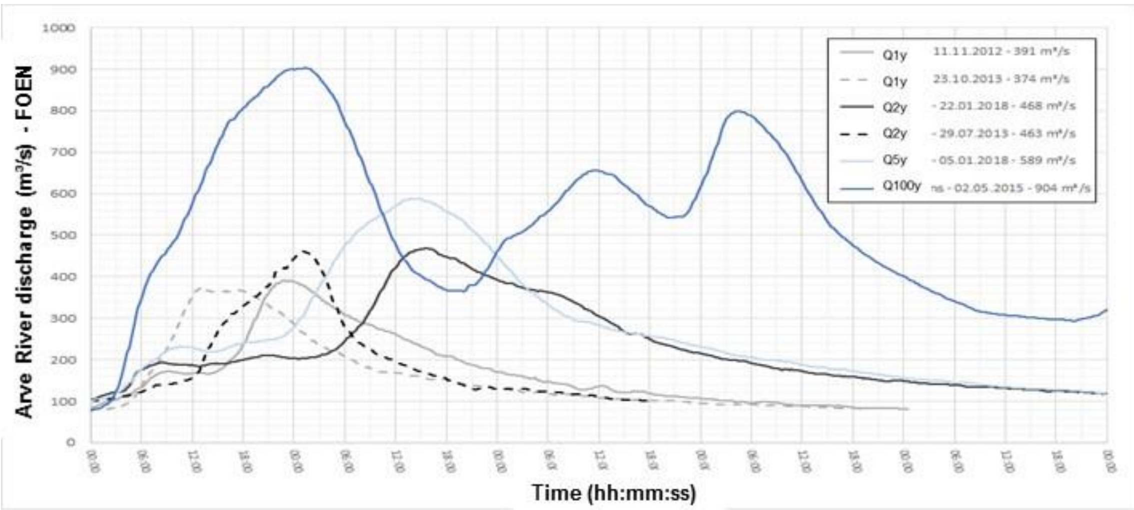

Figure 6 Flood hydrographs for different return periods, FOEN data records

3.2 Biological data

Five fish target species were identified out of twenty inventoried in the Arve River. They are as followed: Brown trout (*Salmo trutta fario*, L.), Lake trout (*Salmo trutta lacustris*, L.), Grayling (*Thymallus thymallus*, L.), Chub (*Leusiscus cephalus*, L.), Barbel (*Barbus barbus*, L.). The migration period of each of them is shown in Figure 7, and related to the hydrological regime of Arve River. Low-flow conditions characterise the migration period of brown and lake trouts. Snow melting generates high suspended sediment load concentration during that of the three other target species. The fish pass structure has to enable upstream migration of the target species, no matter their developmental stage nor their swimming and jumping ability.

Figure 7 Hydrological regime of Arve River, and migration periods of the five target species.

3.3 Sediment data

Suspended sediment transport data has been recorded by the SIG on the site of the federal hydrological station of Bout-du-monde. While these data helped calibrating a numerical hydraulic model (not the subject of the present paper), they could not be directly exploited for the physical modelling, where clogging potential due to fine sediment may be estimated by $KMnO_4$ colour dye dispersion.

Weak bed load data are available on the Geneva reach of the Arve River. The watershed, composed of steep mountain streams, constitutes the sediment production area. Due to snow melt, the daily high-water is accompanied with heavy suspended load with a concentration higher than 1 g/l. The alluvial river conveys an annual suspended sediment volume of 700’000 m³/y and an annual bed load of about 15’000 m³/y.

Although annual bed load discharge is estimated by the SIG, it could not be exploited for modelling purposes on a time scale of flooding events. The Laboratory for Applied Hydraulics therefore carried out bed grain distribution sampling on 11 sites of the Vessy meander which yielded 14 sediment samples. Arve River bed-grain distribution curves obtained from field sampling by the Laboratory for Applied Hydraulics of HEPIA are presented in Figure 8.

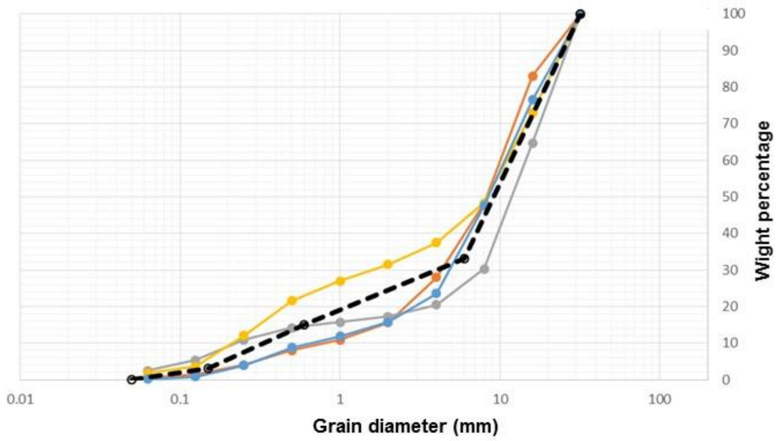

Figure 8 Arve River bed grain distribution curves obtained by the Laboratory by sampling of the Vessy meander

4 EXPERIMENTAL SETUP

4.1 Model extent

The overall extent of the physical hydraulic model of Vessy is presented in the Figure 9. The water inlet of the model is situated 350 m (prototype) upstream from the Vessy spillway. The downstream hydraulic control section is defined some 300 m downstream from the power plant. These boundaries define an about 800 m long river reach. The 680 x 380 m overall prototype dimensions require a 17.0 x 9.5 m floor space in the Laboratory (1:40 geometrical scale). The considered prototype topography extends between the altitudes of 393 and 395 MASL. The overall screed of the model culminates at 400 MASL, preventing overflow in the Laboratory. The topography of Vessy is modelled by means of mortar, faithfully replicating the digital elevation model (SITG). The model of all hydraulic works are made of PVC, with mobile and removable elements allowing quick adaptations for scenario modelling. The movable river bed is modelled by calibrated sand (cf. Figure 11).

Water is conveyed on the model by the closed-loop network of the Laboratory. The model is placed 1.20 m above the laboratory floor, in order to allow a gravitational outlet to the 54 m³ retention basin situated downstairs. Three centrifugal pumps allow to covey a 0.150 m³/s maximum water discharge (0.050 m³/s each). At the upstream boundary, water emerges from a stilling basin. Sediment is also supplied at this point. At the downstream boundary of the model a second stilling and sedimentation basin helps bed load recovery.

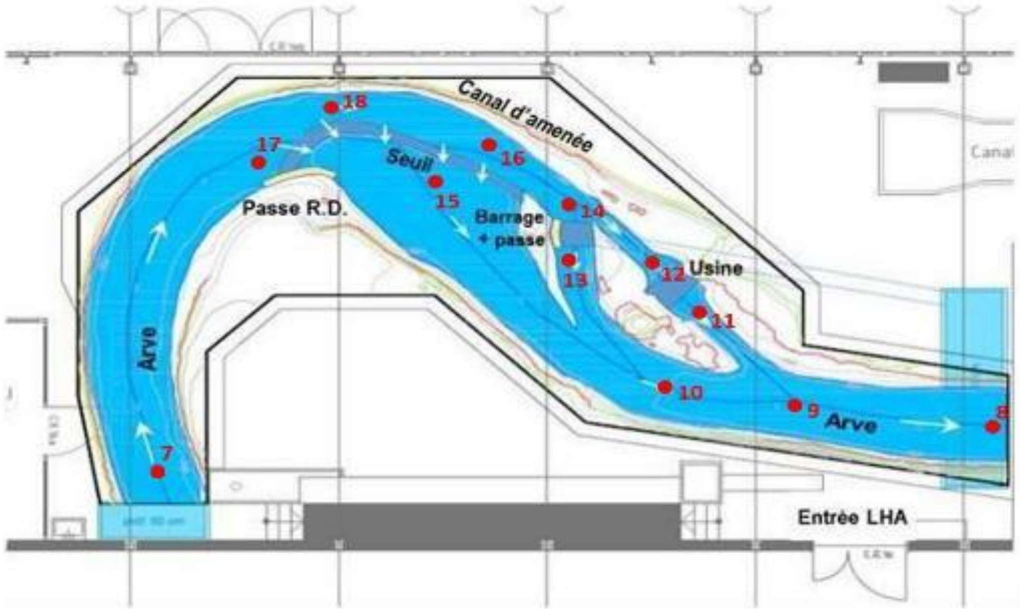

Figure 9 Model extent of the Vessy meander, in the Laboratory for Applied Hydraulics of HEPIA. Dotes indicate the location of ultrasound level probes on the model.

4.2 Model scaling laws

The physical hydraulic model of the Vessy was constructed with a 1:40 geometrical scale. It obeys the Froude similarity law assuming the conservation of ratio between inertial and gravity forces. The scaling factors of the primary physical parameters are presented in Table 1.

Table 1 Model scaling laws for different hydraulic variables, obeying Froude similarity, with λ = 40 geometry scale. Index **p** for prototype, **m** for model.

Physical parameters	Scaling ratio	Scaling factor
Length, L (m) Pressure, P (m water column)	$\frac{L_p}{L_m} = \frac{P_p}{P_m} = \lambda$	40
Velocity, V (ms^{-1}) Time, t [s]	$\frac{V_p}{V_m} = \frac{t_p}{t_m} = \lambda^{1/2}$	6.32
Discharge, Q (m^3s^{-1})	$\frac{Q_p}{Q_m} = \lambda^{5/2}$	10’119
Roughness, K ($m^{1/3}s^{-1}$)	$\frac{K_m}{K_p} = \lambda^{1/6}$	1.849

4.3 Bed load similarity

For the sediment transport analyses, the physical model is exploited under bed load similarity, on the basis of the flowing hypotheses:

i. Sediments are composed of non-cohesive grain material and characterised by their specific mass and mean grain diameter, d_m.
ii. The mean grain diameter and grain size distribution of the natural river sediments were obtained by sampling carried out by the Laboratory on site (cf. Section 3.3 and Figure 8).
iii. The model grain-size distribution was defined due to two similarity laws: the initiation of bed grain motion due to Shields criteria and the bed instability criteria due to roughness Reynolds number, Re*.

iv. Wall roughness of the model has been fitted on the bases of Swiss Federal hydrological data and backwater profile simulation.

4.4 Boundary conditions

The upstream water inflow discharge is monitored by an electromagnetic flowmeter coupled with an electric valve. The appropriate discharge is piloted by an *ad hoc* LabVIEW program, enabling the simulation of any chosen hydrograph. The sediment load calibrated to the hydrograph is released on the model by a conveyor belt obeying the LabVIEW program, surmounted by a sediment tank. At the upstream boundary, the subcritical flow condition is achieved by means of a stilling basin yielding a uniform inflow pattern over the channel cross-section. A calibrated orifice-weir device ensures the downstream hydraulic boundary condition. Due to the Vessy spillway, discharge is first diverted between the inlet canal of the power plant and the main river stream. Further discharge splitting are due to the hydraulic structures of the plant. Ultrasound probes yield water level monitoring at distinct measurement points of the model as presented in Figure 9. The applied physical-parameter measurement techniques and their uncertainties are shown in Table 2.

Table 2 Primary measurement techniques and their uncertainty

Physical parameter	**Measurement technique**	**Uncertainty**
Level	Automatic ultrasound probe (Unam)	1 mm
Morphology, bathymetry	Rotating laser scanner (Leica P16)	0.8 mm à 10m
Water discharge	Electromagnetic flow meter (E+H)	1% of max discharge

5 MODEL CALIBRATION

5.1 Hydraulics

The physical model was calibrated from a hydraulic point of view with a series of steady state water discharges, 20, 40, 100, 200, 482 (T=2y), 600 (T=5y) and 685 m³/s (T=10y) - prototype values.

Figure 10 Flood simulation examples for T=5y and T=10y events, on the Vessy physical model

5.2 Sediment

Sediment transport calibration was achieved on the physical model by respecting Shields similarity law and Reynolds grain roughness criteria.

- The equivalence for the dimensionless shear stress, Θ^* (Eq. [1]), is achieved on the physical model, by obeying Shields criteria for sediment motion / no motion.

$$\Theta^* = \frac{\rho\, g\, R_H\, J}{g\,(\rho_S - \rho)\, d_{90}} \qquad [1]$$

where

ρ (kg/m³), specific mass of water,
ρ_S (kg/m³), specific mass of dry bed sediment,
g (m/s²), acceleration due to gravity,
R_H (m), hydraulic radius,
J (-), flow energy slope,
d_{90} (m), armoured bed grain size.

- The bed grain roughness, expressed in Eq. [2] by the particle Reynolds number, Re*, needs to place the model in the same bed pattern regime as on the prototype, which is pointed out in Table 3.

$$\mathrm{Re}^* = \frac{u^*\, d_{90}}{\nu} \qquad [2]$$

where

u* (-),	dimensionless shear velocity;
ν (m²/s),	kinematic viscosity of water,

with

$$u^* = \sqrt{g\, R_H\, J} \qquad [3]$$

Table 3 Hydraulic variables expressed as a function of bed grain roughness Re* and shear stress θ* for the prototype and the physical model

	T (years)	d (mm)	Q m³s⁻¹	h (m)	Re* (-)	Θ* (-)	Regime
Prototype	30	32	785	3.17	14'020	1.482	Antidunes
Model	30	5	0.078	0.079	346	1.482	Transition - Antidunes
Prototype	100	32	880	3.39	55'970	0.210	Antidunes
Model	100	5	0.087	0.085	357	0.210	Transition - Antidunes

Since field data correlating bed load discharge with water discharge do not exist, it had to be determined by experimentation on the physical model. The critical water discharge, Q, corresponding to the initiation of bed load, when $Q_s = 0$, was calculated according to Eq. [4] of Smart & Jaeggi 1983.

$$Q_S = 0 = 2.5\, J^{0.6}\, Q\left(J - \frac{d_m}{12.1\, h}\right) \qquad [4]$$

where

Q_s (m³/s),	sediment load discharge,
Q (m³/s),	water flow discharge,
d_m (m),	mean grain size of bed sediment,
h (m),	flow water depth.

The sediment load of the model could be fitted to the calculated bed load rating curve (see Figure 11).

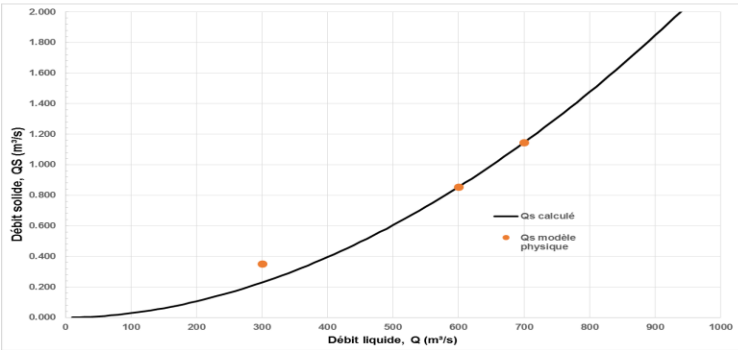

Figure 11 Model bed load, Q_s, expressed as a function of flow discharge, Q, fitted to calculated Q_s(Q) values

6 INITIAL STATE ANALYSIS RESULTS

6.1 Overall comportment

The movable bed physical hydraulic model of the Laboratory for Applied Hydraulics of HEPIA, reproduces accurately the complex hydrodynamic and morphodynamic behaviour of the Vessy meander, as demonstrated by the respective overall views of Figure 12.

Figure 12 Overall view of the Vessy meander. Left: aerial view of the river. Right: the movable bed physical model, in the Laboratory for Applied Hydraulics of HEPIA.

In Figure 13, the detailed views of the alluvial zone and the low-flow channel located downstream from the Vessy spillway demonstrate the accurate comportment of the physical model.

Figure 13 Left: Aerial view of the Vessy meander revealing the alluvial bar and the low flow channel formed downstream from the spillway. **Right**: Simulation result demonstrating the accurate modelling of hydrodynamic and morphologic behaviour of the movable bed physical model.

6.2 The right-bank fish pass

The right-bank fish pass is composed of successive concrete compartments. A convergent flow accompanied by a standing shock wave overtops the (downstream) entrance of the fish pass even by rather weak discharges ($Q=80$ m³/s; T<1y). In order to prevent overtopping and enable fish migration during low and medium water conditions the fish pass had to be protected by vertical panels (see Figure 14).

Figure 14 The fish pass is overtopped by weak flow (T<1y) of Arve, making its entrance inoperative. Bed load deposit upstream from the fish pass and fills up all compartments. **Left**: Arve River. **Right**: physical model.

6.3 Fish pass implementation potential

Since the free fish migration has to be guaranteed along the right bank of the Arve River, the current fish pass suffering from frequent clogging has to be replaced. Feasibility analyses pointed out that a concrete fish pass composed of successive compartments even taking a new path would suffer from clogging. Its construction also happens to be more expensive than that of other techniques. A riprap ramp implemented on the spillway, although less exposed to clogging, would only offer favourable hydraulic conditions by weak and medium discharges of the Arve River. A bypass river appears to gather the largest number of benefits: low clogging risk, flow limitation easily achieved, good environmental potential. The appropriate implementation of its fish entrance and water intake is however key.

Referring to Figure 13, analyses results and field observations, the entrance of the new bypass river appears to be suitable close to the existing one, where the natural stilling basin offers an appropriate water depth. Structural adaptations may however be needed in order to reduce the power to be dissipated in the basin.

Upstream from the Vessy spillway, a sediment point bar extends along the right river bank. Physical modelling pointed out that it lays near beneath the low-water surface level and extends up to 65 meters upstream from the spillway (see Figure 15). Experimental results suggest the location of the future water intake further upstream.

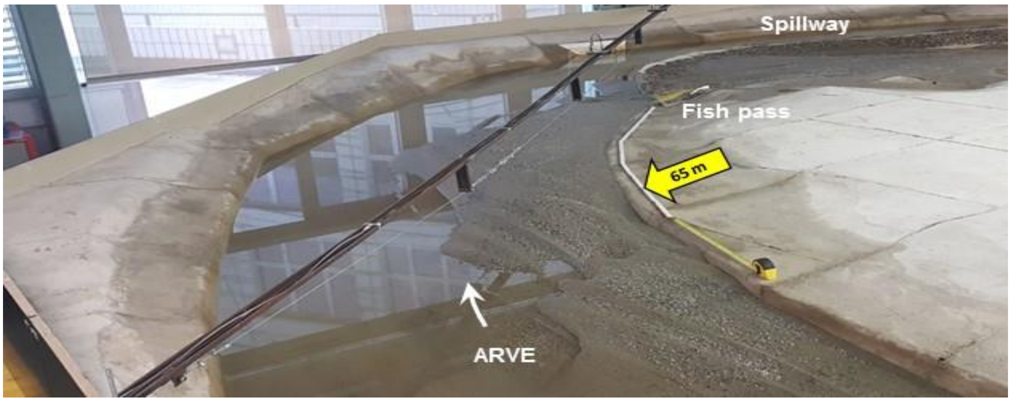

Figure 15 The sediment point bar extends up to 65m (prototype) upstream from the Vessy spillway. The intake of the future bypass river is to be located further upstream, in order to reduce sediment inflow.

7 INVESTIGATION RESULTS

Modelling tests were carried for varying flow conditions of Arve River, different dimensions of the bypass-river intake opening and without / with a groin installed in the Arve (see Figure 16 and Table 4). The hydrodynamic conditions compatible with the swimming competences of all fish target species are guaranteed.

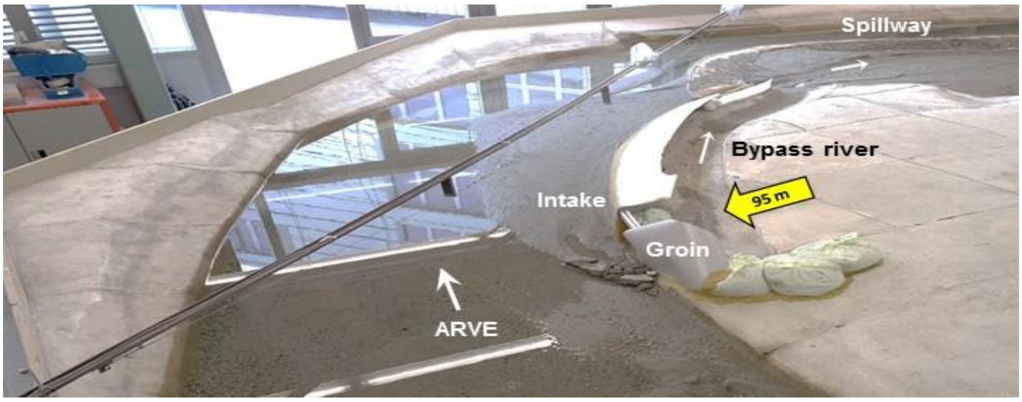

Figure 16 The bypass river on Arve's right bank and a riprap groin in the Arve, implemented on the model.

Table 4 Modelling tests carried out for varying conditions. Intake opening height **a**, width **b**.

T, return period / **Q,** Arve discharge	Intake opening a = 0.75 m, b = 2.5 m **no groin**	Intake opening a = 2.0 m, b = 0.40 m **no groin**	Intake opening a = 0.75 m, b = 2.5 m **GROIN**	Intake opening a = 2.0 m, b = 0.40 m **GROIN**
T (347 days) / 40 m³/s	•	•	•	•
T (30 days) / 150 m³/s	•	•	•	•
T (1 year) / 225 m³/s	•	•	•	•
T (2 year) / 490 m³/s	•	•	•	•
T (10 year) / 690 m³/s			•	•
T (100 year) / 880 m³/s			•	•

In the absence of a groin in the Arve River, the by-pass river filled up with sediment from a Q(2y) flood regardless the dimensions of the intake opening (see Figure 17).

Figure 17 Left: Arve River and the intake device, without a groin. **Right:** Bypass river filled up with sediment, after a Q(2y) test. Intake opening: a=2.0m high, b=0.40m wide (prototype values).

Modelling tests prove that a riprap groin implemented in the Arve River in direct proximity to the intake device, protects efficiently the bypass river from sediment inflow and consequent clogging (see Figure 18) even during a Q(10y) flood of Arve and a 0.75 m high, 2.5 m wide opening of the intake: recommended dimensions.

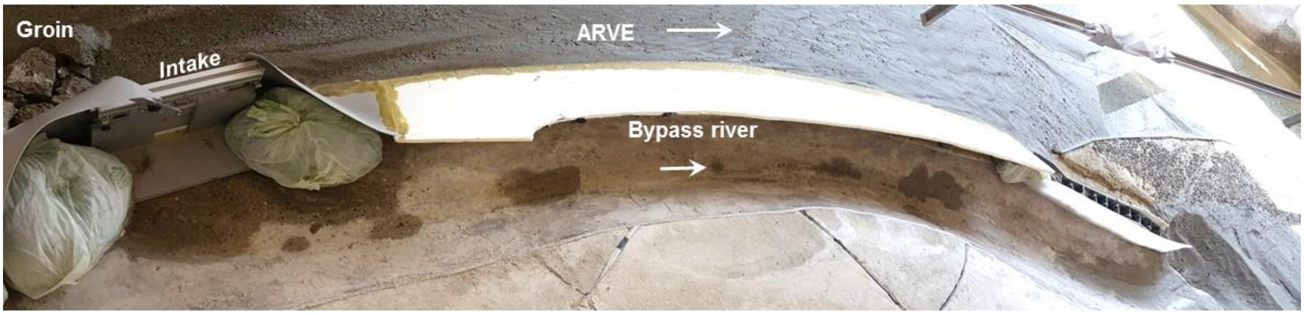

Figure 18 Thanks to the riprap groin implemented in the Arve River, the bypass river remains free from sediment, even after a Q(10y) flood and with a 0.75 m high and 2.50 m wide intake opening (prototype values).

As demonstrated in Figure 18 and Figure 19, the intake device and the associated riprap groin ensure the following functions: a) a clear waterway through the intake opening, b) a clear fish migration connection to Arve's open water even during low-water, c) a low sediment volume conveyed to the bypass river, d) fishes not flushed downstream of the Vessy spillway, once in the open water of Arve.

Figure 19 Left: The intake of the bypass river (a=0.75m, b=2.50m), the riprap groin and its naturally formed stilling basin. **Right:** Even during low-flow of Arve a clear waterway remains to Arve's open water through the intake and the naturally formed stilling basin. The riprap groin prevents efficiently the bypass river from clogging.

8 CONCLUSIONS

An experimental study carried out on a movable bed physical hydraulic model at the Laboratory for Applied Hydraulics of HEPIA yielded a robust solution to replace the right-bank Vessy fish pass suffering from clogging on the Arve River in Geneva. The main achievements of the investigations are:

e) physical model was calibrated to current hydro- and morphodynamic conditions of the Arve River;
f) the bypass river could be defined with a suitable path as well as its entrance and water intake location;
g) the appropriate dimensions of the water intake and the associated riprap groin were identified;
h) the bypass river with its hydraulic structures will guarantee a sustainable solution, free from clogging.

The new fish pass will offer optimal flow and ecological conditions for all fish species and can therefore be constructed at the Vessy meander of the Arve River in Geneva.

REFERENCES

Gren Inventaire piscicole (2009). Concept de gestion et efficacité des mesures. *DGEau, Etat de Genève.*

Gobat, K. (2019). Adaptation des conditions d'écoulement de l'Arve au droit de la passe à poissons rive droite de Vessy – Genève. *HES-SO HEPIA, Bachelor thesis.*

Vecsernyés, Z., Andreini, N., Consuegra, D. Boillat, J-L. (2014). Physical modeling of the third stage of the Aire revitalisation project. *River Fow 2014*.

Vecsernyés, Z., Gobat K., Wohlwend, F. (2019). Rapport intermediaire Vessy I. *Service Industriel de Genève.*

Wohlwend, F. (2015). Etude des conditions d'augmentation du débit turbiné de Vessy-II, par simulation hydraulique numérique. *HES-SO MIT, Mater thesis.*

